Supporting Information (SI) for:

Emissions of ultrafine particles and volatile organic compounds from commercially available desktop 3D printers with multiple filaments

Parham Azimi,[1] Dan Zhao,[1] Claire Pouzet,[1,2] Neil E. Crain,[3] Brent Stephens[1,*]

[1]Department of Civil, Architectural and Environmental Engineering, Illinois Institute of Technology, Chicago, IL USA
[2]Ecole des Ingénieurs de la Ville de Paris (EIVP), 80 Rue Rebeval, 75019 Paris, France
[3]Department of Civil, Architectural, and Environmental Engineering, The University of Texas at Austin, Austin, TX 78712, USA

*Corresponding author:
Dr. Brent Stephens
Civil, Architectural and Environmental Engineering
Illinois Institute of Technology
Alumni Memorial Hall 212
3201 S Dearborn St
Chicago, IL 60616
Phone: (312) 567-3356
Email: brent@iit.edu

30 pages, 23 figures, 4 tables

Table of Contents

1. Experimental setup details

Measurements were conducted inside a 3.6 m^3 chamber (dimensions of 1.2×1.2×2.4 m) located in the Built Environment Research Group Laboratory at the Illinois Institute of Technology. The exterior walls of the chamber were made of 1.1 cm plywood sheets and the interior walls, floor, and ceiling were covered with 0.25 cm stainless steel sheets cut to the same size as the walls, floors, and ceiling. Gaps and edges inside the chamber were sealed with adhesive PTFE film tape (3M 5490). Each printer was tested while operating on a 0.6×0.9×0.9 m stainless steel table at the center of the chamber. A small stainless steel mixing fan was operated to achieve well-mixed conditions in the chamber, which were confirmed prior to the experiments with CO_2 concentration measurements in four locations throughout the chamber. Each printer was connected to a desktop computer located outside the chamber so that it could be operated without opening the chamber door during the test period.

Filtered room air was supplied to the chamber using a 10 cm 12 VDC diameter blower connected to a fibrous activated carbon filter to remove both gases and particulate matter. A DC power supply was used to control the speed of the blower to keep the ventilation rate of the chamber constant near 1 hr^{-1} throughout each test (the ventilation rate was also measured during each test using CO_2 injection and decay as described in the next section). The chamber exhaust port was connected to a 20 cm diameter sheet metal duct that vented directly to a powered fume hood. Figure S1 shows details of the experiment setup.

The interior walls of the chamber were cleaned with distilled water after each experiment and the entire chamber was cleaned with isopropyl alcohol on a weekly basis. The chamber was left unused for at least 2 days after each alcohol cleaning to avoid contamination of VOC samples.

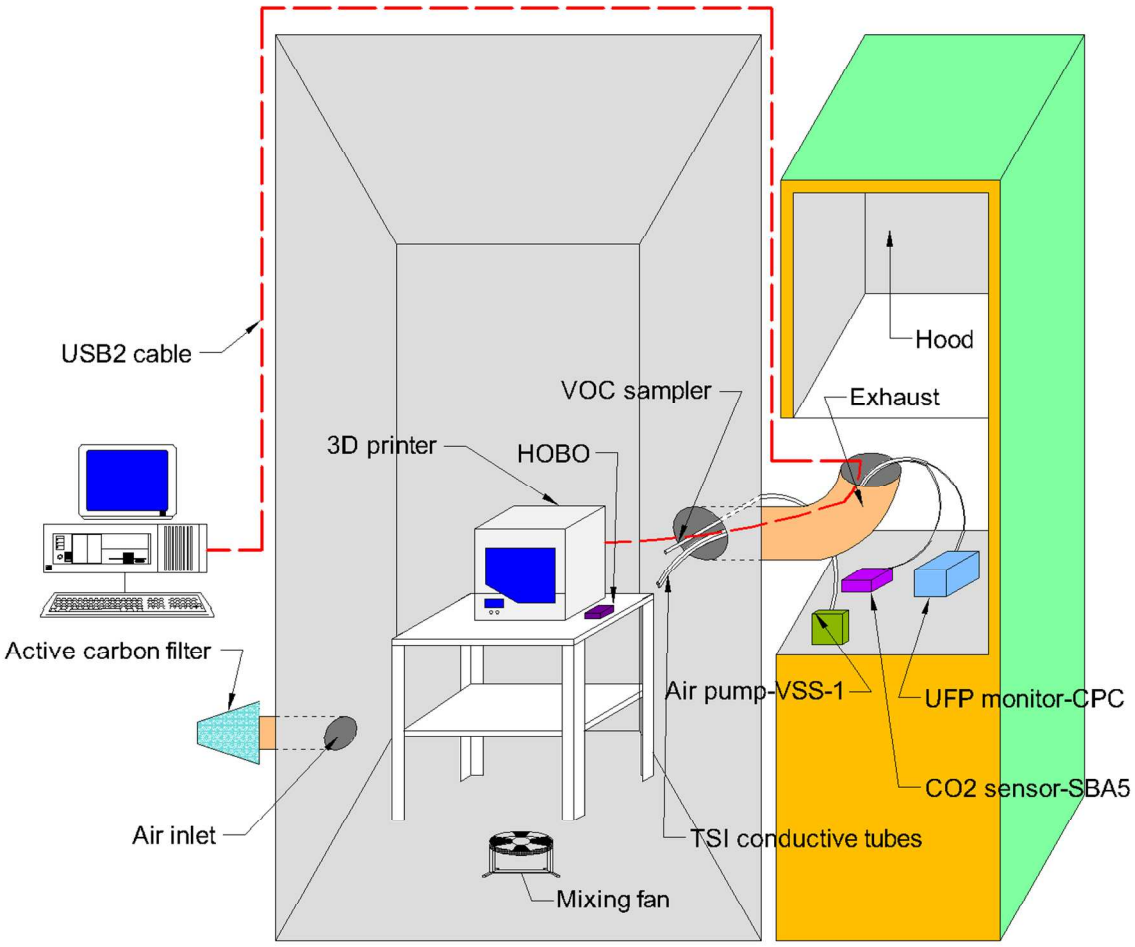

Figure S1: Schematic of the experimental test chamber. All acronyms are defined in the main text.

2. Ventilation rate estimation

We estimated the air exchange rate (AER) of the chamber during each experiment using a CO_2 injection and decay method, which involved increasing the CO_2 concentration inside the chamber by injection from a filtered compressed CO_2 cylinder and measuring the subsequent decay. We applied a dynamic mass balance equation for change in CO_2 concentration inside the chamber as shown in Equation S1.

$$\frac{dC_{co2,in}(t)}{dt} = \lambda C_{CO2,out} - \lambda C_{CO2,in}(t) \quad \text{(S1)}$$

Where
$C_{co2,in}(t)$ = concentration of CO_2 inside the chamber during an experiment (ppm)
t = time (min)
λ = air exchange rate of the chamber during an experiment (1/min)
$C_{CO2,out}$ = concentration of CO_2 outside the chamber during an experiment (ppm)

We also measured the background chamber CO_2 concentrations when it achieved steady state levels prior to the printing experiment and used this value for the concentration outside the chamber. Thus, Equation S1 can be re-written for background period as Equation S2.

$$C_{CO2,out} = \bar{C}_{CO2,in,bg} \quad \text{(S2)}$$

Where
$\bar{C}_{CO2,in,bg}$ = average background CO_2 concentration during an experiment (ppm)

We estimated the AER of the chamber by re-arranging and integrating Equation S1, as shown in Equation S3.

$$-ln\frac{C_{CO2,in}(\mathrm{t}) - \bar{C}_{CO2,in,bg}}{C_{CO2,in}(\mathrm{t}=0) - \bar{C}_{CO2,in,bg}} = \lambda \times t \quad \text{(S3)}$$

We plotted the left hand side of Equation S3 versus time for the first 60 minutes of the decay periods and considered the slope of linear regression line through the data points as the air exchange rate of the chamber during the entire experiment.

3. CPC calibration

We periodically calibrated the TSI Model 3007 Condensation Particle Counter (CPC) used in all experiments via co-location with a TSI Model 3910 NanoScan Scanning Mobility Particle Sizer (SMPS) that had been recently calibrated by the manufacturer. Three printer and filament combinations were operated in the chamber with both monitors logging at 1-minute intervals to provide data for the calibration. Figure S2 shows the raw particle readings from the CPC on the x-axis and the total UFP readings from the SMPS on the y-axis for the three tested combinations of printer and filaments inside the test chamber. Data from the three tests were used to generate a polynomial relationship between the two (R^2 = 0.989). This equation was then applied to all raw CPC concentrations prior to solving for emission rates.

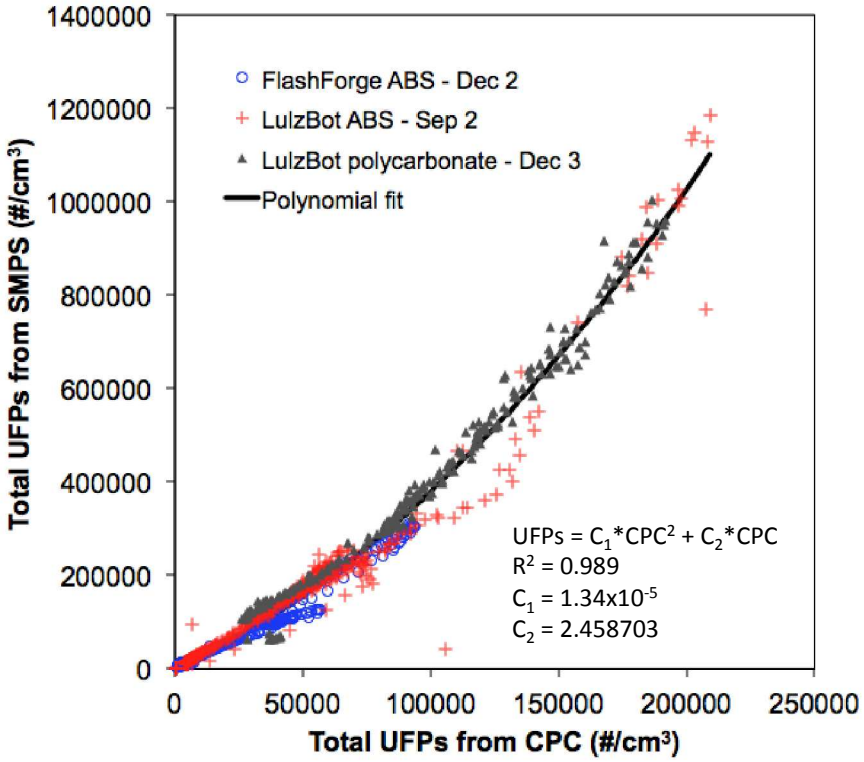

Figure S2: Measured UFP concentration inside the chamber using CPC and SMPS

4. Evaluating the time to reach steady state for TVOCs and the loss rate of TVOCs to chamber walls

TVOC concentrations inside the chamber were continuously measured during a limited subset of experiments using a TSI Q-Trak Indoor Air Quality Monitor Model 7575 with a Model 982 PID-based TVOC probe to verify that TVOC concentrations achieved approximately steady state by the time air sampling for VOC analysis was conducted. As an example, Figure S3 shows time-resolved TVOC concentrations measured during printing the standard NIST sample from using just one printer and filament combination (FlashForge with ABS filament).

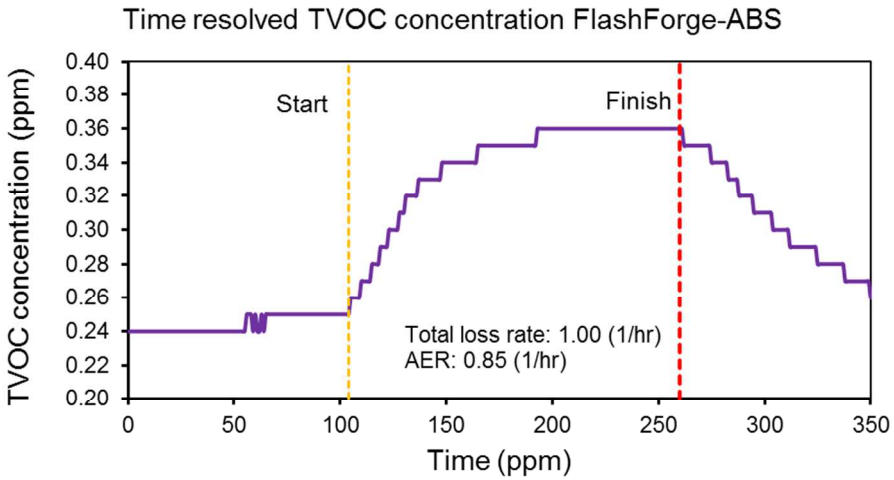

Figure S3: Time resolved TVOC concentration inside the test chamber

Figure S3 shows that the TVOC concentration reached to approximately steady state conditions ~100 minutes after printing started. Two other similar experiments with different printers/filaments were also similar. These measurements verified that approximately steady state conditions were typically achieved within 2 hours from the beginning of printing. Thus we consider air sampling for VOC analysis during the final 45 minutes of printing each object (the printing durations were at least 2 hr 26 min for all experiments) a reasonable assessment of steady state concentrations and can use the difference between the two samples to make reasonable estimates of speciated VOC emission rates.

Additionally, we also used these data to investigate the potential for sorption effects to the stainless steel chamber walls by estimating the total TVOC loss rate from the final decay period in Figure S3 (i.e., after printing stopped around 260 mins). The total TVOC loss rate was approximately 1.0 hr^{-1} using these data while the measured air exchange rate (AER) was 0.85 hr^{-1}. Thus, it appears that in this case, other removal mechanisms such as sorption on the chamber walls may have contributed an additional 0.15 hr^{-1}. However, when we applied the same method to two other experiments the results varied. The total TVOC loss rates were 1.12 and 1.22 hr^{-1}, with corresponding AERs of 1.04 and 1.24 hr^{-1}, respectively. These corresponded with the total loss rate being 7% higher and 2% lower than the chamber air exchange rate. Thus, we consider it reasonable to assume that sorption effects were negligible herein and that ventilation is indeed the major loss mechanism.

5. UFP emission rate estimation

We applied a dynamic well-mixed number balance on the total particle number concentrations measured inside the chamber (Equation S4) to estimate time-varying particle emission rates, which we considered largely representative of UFPs.

$$\frac{dC_{UFP,in}(t)}{dt} = P_{UFP}\lambda C_{UFP,out} - L_{UFP}C_{UFP,in}(\mathrm{t}) + \frac{E_{UFP}(t)}{V} \quad \text{(S4)}$$

where $C_{UFP,in}(t)$ is the UFP concentration inside the chamber at time t (#/m^3), P_{UFP} is the UFP penetration factor of the chamber (-), λ is the air exchange rate of the chamber (1/min), $C_{UFP,out}$ is the UFP concentration outside of the chamber (#/m^3), L_{UFP} is the total UFP loss rate constant inside the chamber (1/min), $E_{UFP}(t)$ is the time-varying UFP emission rate from a single 3D printer at time t (#/min), and V is the chamber volume (m^3).

The UFP concentration inside the chamber prior to testing (i.e., during the background period) reached steady state conditions prior to all experiments. Therefore, the average measured background concentration $\bar{C}_{UFP,bg}$ was used in place of $P_{UFP}\lambda C_{UFP,out}$ using Equation S5.

$$P_{UFP}\lambda C_{UFP,out} = \bar{C}_{UFP,bg}L_{UFP} \quad \text{(S5)}$$

The total UFP loss rate (L_{UFP}) was estimated using a log-linear regression with data from the final decay period after printing finished, as shown in Equation S6. We plotted the left hand side of Equation S6 versus time for the first 60 minutes of the decay period and used the slope of the linear regression as the total UFP loss rate during the entire experiment.

$$-ln\frac{C_{UFP,in}(\mathrm{t}) - \bar{C}_{UFP,bg}}{C_{UFP,in}(\mathrm{t}=0) - \bar{C}_{UFP,bg}} = L_{UFP}t \quad \text{(S6)}$$

Next, we estimated the time-varying UFP emission rate for each 3D printer using a discrete solution to the number balance in Equation S4, as shown in Equation S7.

$$\frac{E_{UFP}(t_{n+1})}{\mathrm{V}} = \frac{\left[C_{UFP,in}(\mathrm{t_{n+1}}) - C_{UFP,in}(\mathrm{t_n})\right]}{\Delta \mathrm{t}} - L_{UFP}\bar{C}_{UFP,bg} + L_{UFP}C_{UFP,in}(t_n) \quad \text{(S7)}$$

where Δt was the time step for UFP measurements (1 min).

We should note that Equations S4 through S7 make several important assumptions that may lead to inaccuracies in estimates of UFP emission rates. We do not consider size-resolved particle dynamics because we did not have access to the SMPS for every test. We assume that particle loss rates were constant throughout each test period, although one would expect them to vary depending on the particle size distribution in the chamber, which may vary at any given time based on size-dependent loss mechanisms such as deposition or coagulation. We have also assumed that the impact of coagulation on total UFP concentrations is negligible, which may not be the case. However, we estimate the likely magnitude of the impact of this assumption on total UFP emission rates to be relatively small (i.e., less than 30%, on average, using the most

conservative estimates of coagulation, as described later herein). While these are important limitations to this work, results can still provide a reasonable quantitative measure of particle emission rates resulting from 3D printer operation that can be used to compare one printer to another.

Further, there was a large amount of scatter in most of the resulting UFP concentration data from one minute to the next, particularly at high concentrations, which led to unreasonable numbers of negative emission rate estimates using the discretized solution method with raw UFP data. This was likely due to high uncertainty beyond the upper limit of the CPC. Therefore, we first applied a smoothing function to the resulting UFP concentration data using the '*smooth*' function in MATLAB R2015a. These smoothed concentration data were then used with Equation S7 to estimate time-varying emission rates with minimal negative values. We applied a number of smoothing function options (e.g., loess, lowess, and others) to each highly varying data set and selected smoothed data from the method that yielded a combination of the fewest negative emission rate estimates and the highest correlation between actual and smoothed UFP concentrations (i.e., R^2 was typically above 0.90, as described later herein). Any remaining periods of negative UFP emission rate estimates, which were likely due to time-varying and size-dependent loss rates that we were not able to account for, were simply excluded from analysis (the average number of negative values excluded was 10 data points out of a total of between ~150 and ~250 data points for each test).

6. VOC emission rate estimation

The TD/GC/MS library compound searches (LCS) identified and quantified approximately 50 speciated VOCs inside the chamber during the initial background periods and at the last ~45 minutes of the printing periods. The estimated mass of each individual VOC was converted to a chamber air concentration using Equation S8.

$$C_{VOC,i} = \frac{m_{VOC,i}}{\bar{Q}_{pump} \times t_{pump}} \quad \text{(S8)}$$

where $m_{VOC,i}$ is the total collected mass of an individual VOC in the sampling tube (μg), $\bar{Q}_{pump}$ is the average sampling pump airflow rate (m^3/min), and t_{pump} is the total VOC sampling time (min) for each sampling period.

Similar to the previous section, we applied a dynamic well-mixed mass balance on the speciated VOC mass concentrations measured inside the chamber, as shown in Equation S9.

$$\frac{dC_{VOC,i}(t)}{dt} = P_{VOC,i}\lambda C_{VOC,i,out} - L_{VOC,i}C_{VOC,i}(\mathrm{t}) + \frac{E_{VOC,i}}{V} \quad \text{(S9)}$$

where $C_{VOC,i}(t)$ is an individual VOC concentration inside the chamber at time t (μg/m^3), $P_{VOC,i}$ is an individual VOC penetration factor of the chamber (-),$C_{VOC,i,out}$ is an individual VOC concentration outside of the chamber (μg/m^3), $L_{VOC,i}$ is the total loss rate constant of an individual VOC inside the chamber (1/min), $E_{VOC,i}$ is the estimated constant emission rate of an individual VOC (μg/min).

Next, the emission rate of each identified VOC was estimated using Equation S10, assuming that ventilation was the only removal mechanism in the chamber, the concentration of 10 top measured emitted VOCs from 3D printers is negligible outside the chamber (verified by measuring individual VOC concentrations outside the chamber), and that VOC concentrations achieved steady state during the final sampling period.

$$E_{VOC,i} = \left(C_{VOC,i,print} - C_{VOC,i\,,bg}\right)\lambda V \quad \text{(S10)}$$

where $C_{VOC,i,print}$ is the steady state concentration of an individual VOC inside the chamber during the last ~45 minutes of printing (μg /m^3), and $C_{VOC,i\,,bg}$ is the background concentration of an individual VOC inside the chamber prior to printing (μg/m^3). We estimated the uncertainty in individual VOC emission rates to be approximately 36% based on the likely uncertainty in the GC/MS quantification method (~25%) combined with the uncertainty in pump flow rate measurements in quadrature (calculated later in Section 8 of the SI). Adsorption and desorption effects were assumed to be negligible given that the interior of the chamber was stainless steel.[1,2] This assumption was further verified by comparing TVOC loss rate estimates from multiple post-printing decay periods measured by the Q-Trak TVOC probe to the air exchange loss rate measured using CO_2 decay, as shown in Section 4 of the SI. Loss rates were similar, suggesting that sorption effects were indeed minor.

7. Impact of coagulation on UFP emission rate estimates

Given that UFP concentrations were often elevated to very high concentrations in the chamber, it is important to consider the potential for particle coagulation to influence our results, even though we did not have size resolved data. Here, we evaluate the likely impact of coagulation on UFP emission rates from the highest UFP emitter in the study: the LulzBot-ABS combination. We used a number balance equation based on our calibrated UFP measurements using the Condensation Particle Counter (CPC). Our assumptions serve to simplify the calculations while maximizing the likely impact of coagulation on estimates of the dynamic UFP emission rate in order to provide an upper bound of the likely impact of neglecting coagulation.

The rate of change of the particle number concentration due to just coagulation can be expressed as Equation S11 for particles with similar aerodynamic diameter:

$$\frac{dC_i(t)}{dt} = -K_{coag}C_i^2(t) \quad \text{(S11)}$$

Where
K_{coag} = corrected coagulation coefficient (cm^3/min)
C_i(t) = number of particles with aerodynamic diameter of i (#/cm^3)

As the CPC measures the number concentration of particles with diameters smaller than 1 µm, we assumed all particles inside the chamber have a similar coagulation coefficient of 6.9×10^{-8} cm^3/min, which is the highest coagulation coefficient for particles smaller than 1 µm.[3] For simplicity, we also assumed that particles collide with just one other particle in each collision and form new particles that are still smaller than 1 µm, which is reasonable given that the majority of particles emitted inside the chamber are smaller than 0.1 µm (demonstrated by early measurements with a combination of TSI Nanoscan SMPS Nanoparticle Sizer 3910 and TSI Optical Particle Sizer 3330, as shown in Figure S4).

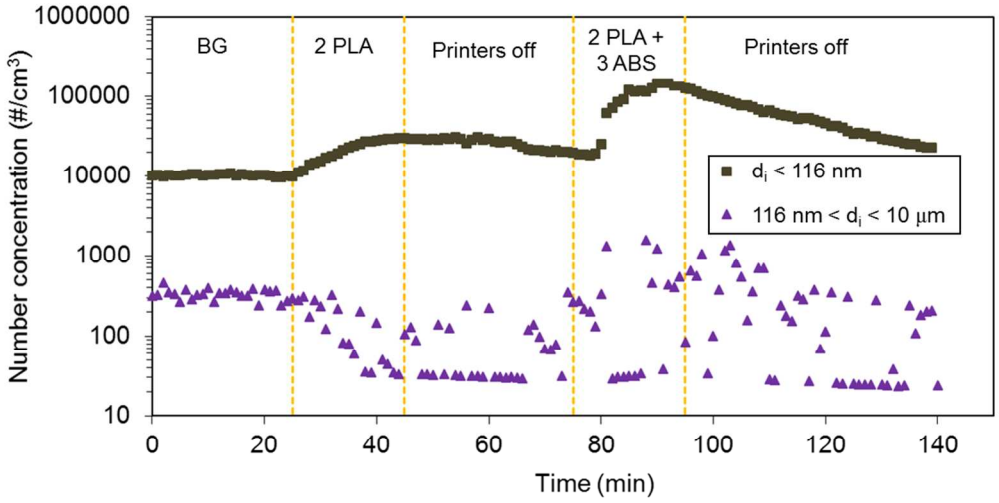

Figure S4: Comparison of total number concentration of particles smaller than 116 nm and between 116 nm and 10 µm in the Stephens et al. (2013) study

Figure S4 compares the total number concentration of particles smaller than 116 nm to those summed between 116 nm and 10 μm inside an office environment in downtown Chicago.[4] Five time periods are defined: (1) background measurements without printers operating for approximately 25 min; (2) two identical 3D printers using PLA filament operating for approximately 20 min; (3) a time period of approximately 30 minutes in which all printers were turned off; (4) the same two PLA-based printers operating simultaneously with three of the same make and model printers operating with ABS filament for approximately 20 min; and (5) a concentration decay period lasting approximately 40 min. The results demonstrate that the vast majority of particles emitted during printing are smaller than 116 nm (i.e., UFPs).

Therefore, the number balance equation for particles inside the chamber considering coagulation can be written as Equation S12.

$$\frac{dC_{UFP,in}(t)}{dt} = P_{UFP}\lambda C_{UFP,out} - L_{UFP}C_{UFP,in}(\mathrm{t}) + \frac{E_{UFP}(t)}{V} - \frac{1}{2}K_{coag}C_{UFP,in}^2(t) \quad \text{(S12)}$$

$C_{UFP,in}$= total concentration of UFPs inside the chamber (#/cm^3)
P_{UFP} = UFP penetration factor of chamber (-)
$C_{UFP,out}$= total concentration of UFPs outside the chamber (#/cm^3)
L_{UFP}= UFP loss rate inside the chamber due to AER and deposition (1/min)
$E_{UFP}(t)$ = emission rate of UFP from 3D printer (#/min)
V = chamber volume (cm^3)

We assumed that during the background period there was no UFP emission source inside the chamber and that UFP concentrations reached steady state conditions. Therefore, the number balance equation for background periods can be written as Equation S13.

$$\frac{P_{UFP}\lambda C_{UFP,out}}{L_{UFP}} = C_{UFP,bg} + \frac{K_{coag}}{2L_{UFP}}\, C_{UFP,bg}^2 \quad \text{(S13)}$$

In this equation $P_{UFP}\lambda C_{UFP,out}$ and L_{UFP} are unknown. We then used a dynamic number balance equation for the decay period, as shown in Equation S14, in which we assumed that the emission of particles from 3D printers stopped completely after the printing period.

$$\frac{dC_{UFP,in}(t)}{dt} = P_{UFP}\lambda C_{UFP,out} - L_{UFP}C_{UFP,in}(\mathrm{t}) - \frac{1}{2}K_{coag}C_{UFP,in}^2(t) \quad \text{(S14)}$$

Equation S14 can be solved by taking an integral as shown in Equation S15.

$$\int_{C_{UFP,in}(t=0)}^{C_{UFP,in}(t)} \frac{dC_{UFP,in}(t)}{\frac{K_{coag}}{2L_{UFP}}C_{UFP,in}^2(t) + C_{UFP,in}(\mathrm{t}) - \frac{P_{UFP}\lambda C_{UFP,out}}{L_{UFP}}} = \int_0^t -L_{UFP}dt \quad \text{(S15)}$$

Using a trial and error method, we estimated the UFP loss rate due to AER and deposition (L_{UFP}) combined, as follows:

- First, we chose a reasonable value for L_{UFP} without considering coagulation with the same method as described in Equations S4-S6 in Section 5.
- Second, we calculated $\frac{K_{coag}}{2L_{UFP}}$ and $\frac{P_{UFP}\lambda C_{UFP,out}}{L_{UFP}}$ values in Equation S15 by knowing the average UFP concentration during the background period.
- Third, we plotted the left hand side values of Equation S15 versus time for the first 60 minutes of the decay periods and considered the slope of linear regression line assigned to the data points as L_{UFP}. The left hand side values were calculated using MATLAB R2015a.
- Finally, we compared the calculated UFP loss rate and the value we chose at the first step. We ended the trial and error cycle once the two values were within 0.001 1/min of each other; otherwise, we used the new estimation of UFP loss rate due to AER and deposition in the first step and repeated the trial and error solution.

We estimated the time-varying UFP emission rate with and without considering coagulation using a discrete solution to the number balance in Equation S12, similar to the solution described in Equation S7. Figure S5 shows estimates of time resolved UFP emission rates from the LulzBot-ABS combination with and without considering coagulation in this manner.

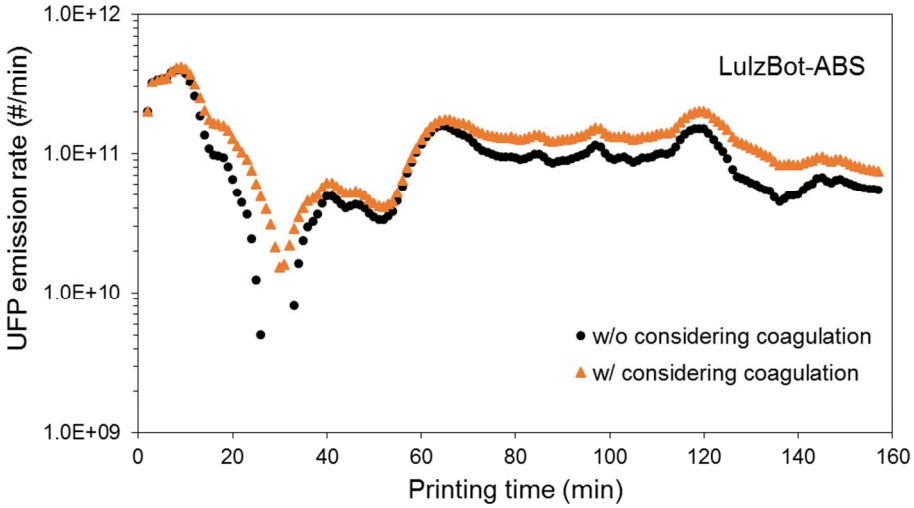

Figure S5: Comparison between UFP emission rate estimations with and without considering coagulation

In this analysis, although we assumed the highest coagulation coefficient for particles less than 1 μm, and considered the printer and filament combination with the highest average UFP concentration during printing period, the mean impact of coagulation was ~28% (changing from -1% to 90%). The average difference between estimated UFP emission values with and without considering coagulation was ~3×10^{10} #/min (ranges from -3×10^{9} to 7×10^{10} #/min) which is about an order of magnitude smaller than average estimated UFP emission, (~10^{11} #/min). The results demonstrate that although the coagulation might impact the UFP emission rate estimates, specifically for the highest concentrations of UFPs, the impact is likely smaller in most cases and generally within the uncertainty of our estimates. Thus we consider it reasonable to neglect coagulation impacts herein.

8. Uncertainty analysis

We estimated the uncertainty in our UFP and VOC emission rate estimates using a variety of approaches. First, we calculated the uncertainty in each smoothed concentration of UFP data, the average background concentration of UFPs, the chamber air exchange rate (AER), and the total UFP loss rate by adding standard errors of regression coefficients from related equations and the accuracy of each monitoring device in quadrature.

The uncertainty associated with the smoothed concentration of UFP is a function of the reported accuracy of the TSI CPC model 3007 (±20%) and the standard error due to both calibration (R^2_{calib} = 0.981) and smoothing (R^2_{smooth} > 0.9, varied depend on the experiment), which was calculated using Equation S16.

$$\Delta C_{UFP,smooth} = \sqrt{(AC_{CPC})^2 + \left(\frac{SE_{UFP,calib}}{\bar{C}_{UFP,calib}}\%\right)^2 + \left(\frac{SE_{UFP,smooth}}{\bar{C}_{UFP,smooth}}\%\right)^2} \quad \text{(S16)}$$

Where:

$\Delta C_{UFP,smooth}$ = uncertainty associated with smoothed UFP concentration inside the chamber for each combination of 3D printer, filament and printing object shape (%)

AC_{CPC} = average accuracy of TSI CPC model 3007 (±20%)

$SE_{UFP,calib}$ = standard error of the calibration (± 933 #/cm^3)

$\bar{C}_{UFP,calib}$ = average concentration of UFP inside the chamber during the calibration measured by SMPS (± 183444 #/cm^3)

$SE_{UFP,smooth}$ = standard error of the smoothing procedure for each studied combination (#/cm^3)

$\bar{C}_{UFP,smooth}$ = average smoothed concentration of UFP inside the chamber during the printing period for each studied combination (#/cm^3)

The uncertainty associated with the background concentration of UFPs is a function of the average accuracy of the CPC, the standard error of the mean, and the standard error due to calibration, which was calculated using Equation S17.

$$\Delta C_{UFP,bg} = \sqrt{(AC_{CPC})^2 + \left(\frac{SE_{UFP,calib}}{\bar{C}_{UFP,calib}}\%\right)^2 + \left(\frac{SE_{UFP,bg}}{\bar{C}_{UFP,bg}}\%\right)^2} \quad \text{(S17)}$$

Where

$\Delta C_{UFP,bg}$ = uncertainty associated with average background UFP concentration inside the chamber for each combination of 3D printer, filament and printing object shape (%)

$SE_{UFP,bg}$ = standard error of the mean background UFP concentration inside the chamber for each studied combination (#/cm^3)

$\bar{C}_{UFP,smooth}$ = average background concentration of UFP inside the chamber during the printing period for each studied combination (#/cm^3)

We estimated the air exchange rate of the chamber from Equations S1-S3 using a CO_2 inject-decay method. The uncertainty associated with the AER of chamber is a function of the average accuracy of SBA-5 CO_2 anazlyer, the standard error of the mean CO_2 background, and the standard error due to fitting a linear regression line to the left hand side (LHS) of Equation S3, which was calculated using Equation S18.

$$\Delta AER = \sqrt{\left(\frac{AC_{SBA5}}{\bar{C}_{CO2,decay}}\%\right)^2 + \left(\frac{AC_{SBA5}}{\bar{C}_{CO2,bg}}\%\right)^2 + \left(\frac{SE_{CO2,bg}}{\bar{C}_{CO2,bg}}\%\right)^2 + \left(\frac{SE_{CO2,LHS}}{\overline{LHS}_{CO2}}\%\right)^2} \quad \text{(S18)}$$

Where
ΔAER = uncertainty associated with AER of the chamber for various experiments (%)
AC_{SBA5} = average accuracy of SBA5 CO_2 monitor (± 20 ppm)
$\bar{C}_{CO2,decay}$ = average concentration of CO_2 during the decay period for each experiment (ppm)
$\bar{C}_{CO2,bg}$ = average concentration of background CO_2 for each experiment (ppm)
$SE_{CO2,bg}$= standard error of the mean CO_2 background concentration for each experiment (ppm)
$SE_{CO2,LHS}$= standard error of linear regression line fitted to left hand side values of Equation S3 to estimate AER for each experiment (-)
$\overline{LHS}_{CO2}$ = left hand side values average in Equation S3 to estimate AER for each experiment (-)

We also estimated the uncertainty associated with the total loss rate for each combination of printer, filament, and printing object shape based on the regression coefficients from Equation S6 in Section 5. The total loss rate uncertainty is a function of the background and smoothed UFP concentrations and the standard error of the linear regression between to the left hand side (LHS) of Equation S6 versus time, which was calculated using Equation S19.

$$\Delta L_{UFP} = \sqrt{\left(\Delta C_{UFP,smooth}\right)^2 + \left(\Delta C_{UFP,bg}\right)^2 + \left(\frac{SE_{UFP,LHS}}{\overline{LHS}_{UFP}}\%\right)^2} \quad \text{(S19)}$$

ΔL_{UFP} = uncertainty associated with the UFP loss rate for various experiments (%)
$SE_{UFP,LHS}$= standard error of linear regression line fitted to left hand side values of Equation S6 to estimate UFP total loss rate for various experiments (-)
$\overline{LHS}_{UFP}$ = average of left hand side values in Equation S6 to estimate UFP total loss rate for various experiments (-)

Finally, we estimated the uncertainty associated with the air flow rate of the VOC sampling pumps. For each VOC sampling tube and pump combination, we measured the air flow rate through the tube five times, and calculated the uncertainty in this airflow rate as a function of the average accuracy of the air flow meter and the standard error of the mean measured air flow rate, as shown in Equation S20.

$$\Delta Q_{pump} = \sqrt{\left(\frac{AC_{flowmeter}}{\bar{Q}_{pump}}\%\right)^2 + \left(\frac{SE_Q}{\bar{Q}_{pump}}\%\right)^2} \quad \text{(S20)}$$

Where

ΔQ_{pump} = uncertainty associated with air flow passing through VOC sampling tubes (%)

$AC_{flowmeter}$= average accuracy of air flow meter (± 1 cm^3/min)

$\bar{Q}_{pump}$ = average air flow passing through VOC sampling tubes (cm^3/min)

SE_Q = Standard error of mean measured air flow passing through VOC sampling tubes (cm^3/min)

Next, we used the previous uncertainty estimations to calculate uncertainty associated with time varying UFP emission rate, VOC concentration in background and printing periods, and VOC emission rate from each printer. We calculated the uncertainty of time-varying UFP emission rates based on Equation S7, as shown in Equation S21.

$$\Delta E_{UFP}(t_{n+1}) = \sqrt{\left(\Delta C_{UFP,in}(t_{n+1})\right)^2 + \left(\Delta C_{UFP,in}(t_n)\right)^2 + (\Delta L_{UFP})^2 + \left(\Delta \bar{C}_{UFP,bg}\right)^2} \quad \text{(S21)}$$

Where

$\Delta E_{UFP}(t_{n+1})$ = uncertainty associated with UFP emission rate (%)

We calculated the uncertainty of VOC concentration in background and printing periods based on the Equation S8 in Section 6, as shown in Equation S22.

$$\Delta C_{VOC} = \sqrt{\left(AC_{M,VOC}\right)^2 + \left(\Delta Q_{pump}\right)^2} \quad \text{(S22)}$$

Where

ΔC_{VOC} = uncertainty associated with VOC concentration in background and printing periods (%)

$AC_{M,VOC}$ = Accuracy of GC-MS technique to quantify collected mass of VOC in the sampling tubes (assumed to be ± 25% for a typical relative response factor between 0.75 and 1.25)

Finally, we calculated the uncertainty in the VOC emission rate estimate based on the Equation S10 in Section 6, as shown in Equation S23.

$$\Delta E_{VOC,i} = \sqrt{\left(\Delta C_{VOC,i,print}\right)^2 + \left(\Delta C_{VOC,i,bg}\right)^2 + (\Delta \mathrm{AER})^2} \quad \text{(S23)}$$

Where

$\Delta E_{VOC,i}$ = uncertainty associated with estimated VOC emission for each component (%)

9. Time varying UFP concentration data and estimated emission rates

As described briefly in the main text, we applied a number of smoothing function options (e.g., loess, lowess, and others) to each highly varying data set and selected smoothed data from the method that yielded a combination of the fewest negative emission rate estimates (fewer than 5%) and the highest correlation between actual and smoothed UFP concentrations (R^2 was mostly above 0.90). However, in four case studies (i.e. LulzBot-HIPS, LulzBot-Nylon, LulzBot-TGlase, and FlashForge-ABS) the number of negative estimated emissions were higher than 5%, as shown in the following figures. The negative emission estimations may be due to a combination of coagulation impacts and UFP loss rate underestimation. In most of the cases, the negative emission estimations were happened during high concentrations of UFP (~10^5 #/cm^3 and higher), where the coagulation impacts are considerable. In Section 7 we demonstrated that without considering coagulation we might underestimate the emission estimations up to 90% at UFP pick concentrations in extreme case scenarios, although in average, the impacts would be lower than 28%, specifically for low UFP emitter combinations of printer and filament. Moreover, in the all four cases the loss rates were estimated when the UFP concentrations in decay period were about three orders of magnitude lower than the corresponding UFP pick concentrations. This might cause an underestimation in particle loss rates due to changes in particles' size distribution and deposition rate.

We used the *'smooth'* function in MATLAB-R2015a with various smoothing methods (SM), as shown in Table 1.

Table S1: Description of various smoothing methods used herein

method	Description
'moving'	Moving average (default). A lowpass filter with filter coefficients equal to the reciprocal of the span.
'lowess'	Local regression using weighted linear least squares and a 1st degree polynomial model
'loess'	Local regression using weighted linear least squares and a 2nd degree polynomial model
'sgolay'	Savitzky-Golay filter. A generalized moving average with filter coefficients determined by an unweighted linear least-squares regression and a polynomial model of specified degree (default is 2). The method can accept nonuniform predictor data.
'rlowess'	A robust version of 'lowess' that assigns lower weight to outliers in the regression. The method assigns zero weight to data outside six mean absolute deviations.
'rloess'	A robust version of 'loess' that assigns lower weight to outliers in the regression. The method assigns zero weight to data outside six mean absolute deviations.

Figures S6(a) - S23(a) show calibrated and smoothed UFP concentrations inside the chamber, nozzle and bed temperatures during printing, smoothing method (SM), coefficient of determination between smoothed and calibrated data (SM-R^2), and our estimate of the total UFP loss rate. Figures S6(b) - S23(b) show the estimates of time-varying UFP emission rates during each printing period as well as the number of negative estimated emissions (NNEE) for all tested combinations.

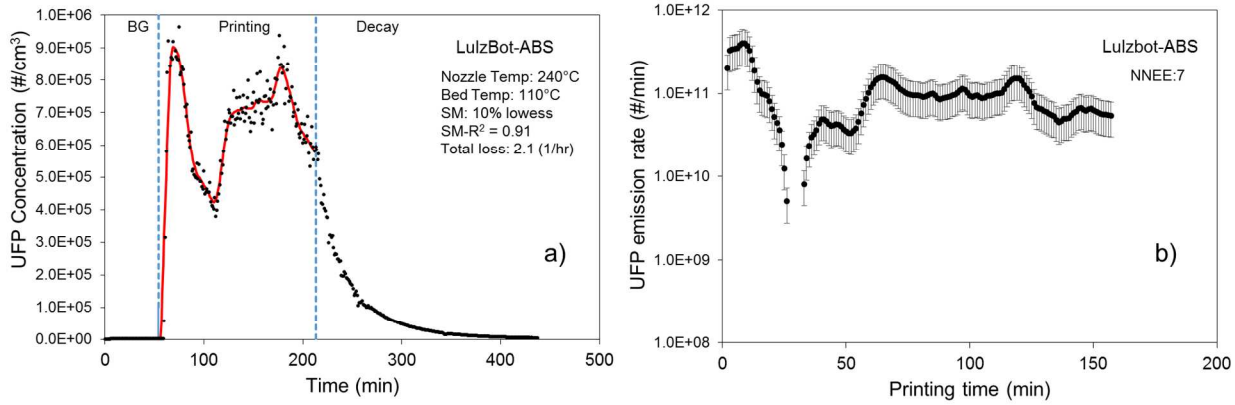

Figure S6: (a) Calibrated and smoothed UFP concentration inside the chamber and (b) Time varied UFP emission rate for LulzBot-ABS

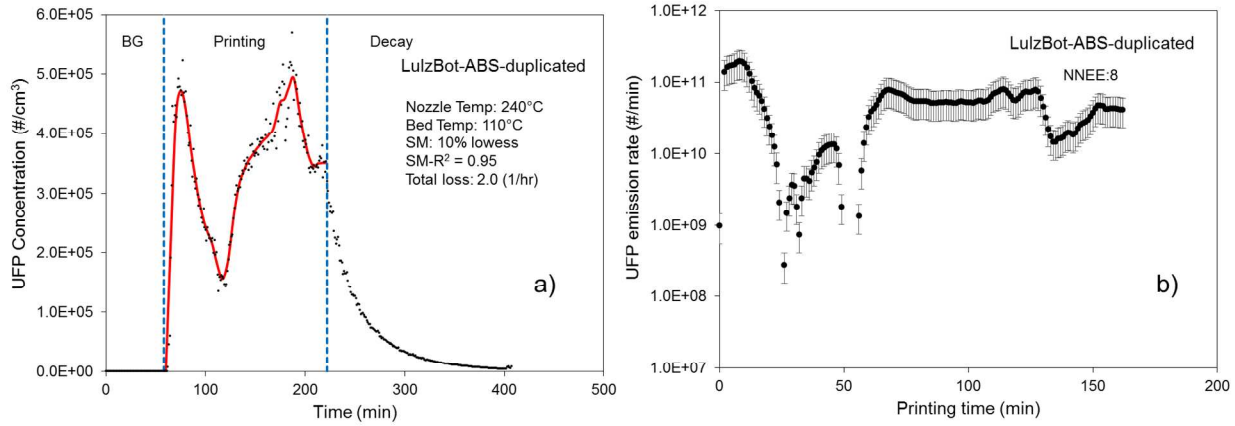

Figure S7: (a) Calibrated and smoothed UFP concentration inside the chamber and (b) Time varied UFP emission rate for LulzBot-ABS (Duplicated)

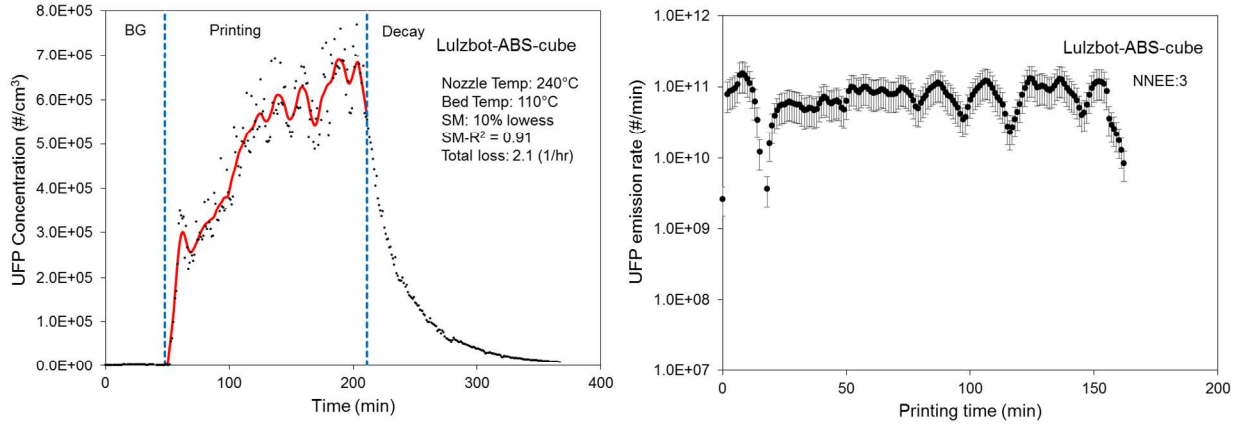

Figure S8: (a) Calibrated and smoothed UFP concentration inside the chamber and (b) Time varied UFP emission rate for LulzBot-ABS (Cube)

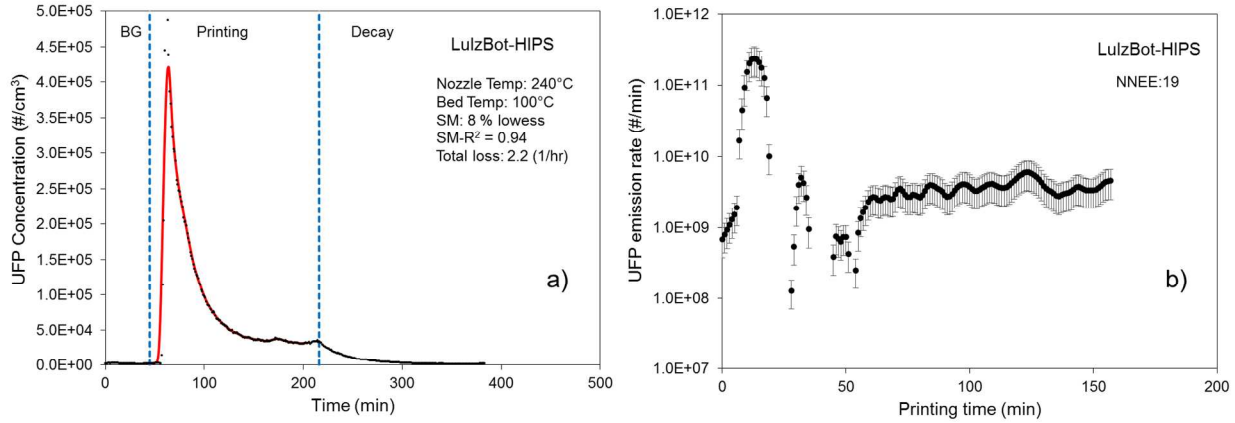

Figure S9: (a) Calibrated and smoothed UFP concentration inside the chamber and (b) Time varied UFP emission rate for LulzBot-HIPS

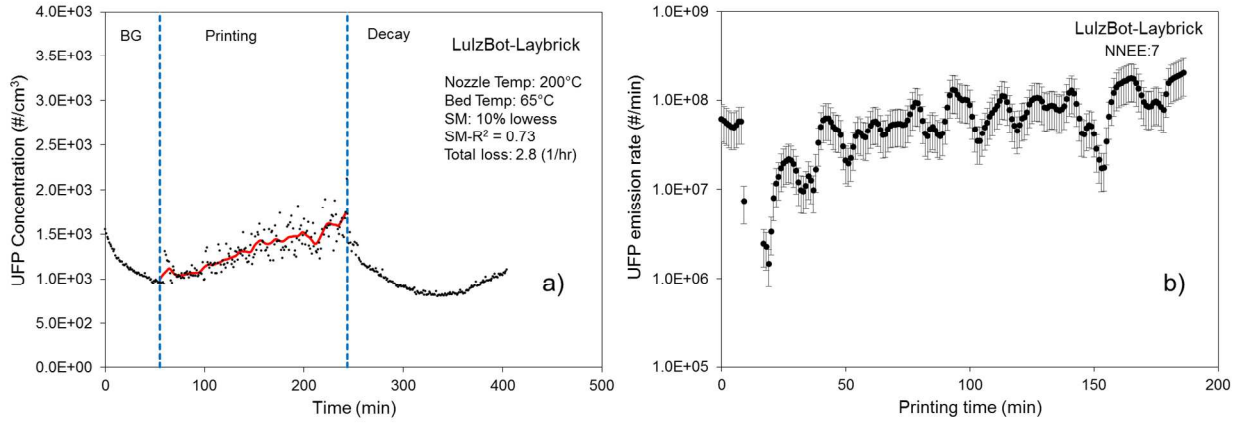

Figure S10: (a) Calibrated and smoothed UFP concentration inside the chamber and (b) Time varied UFP emission rate for LulzBot-Laybrick

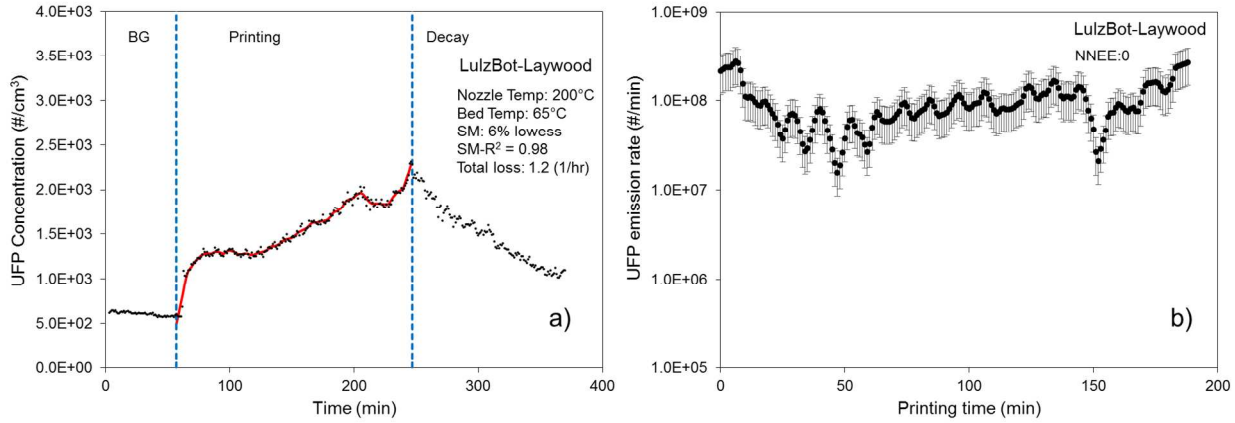

Figure S11: (a) Calibrated and smoothed UFP concentration inside the chamber and (b) Time varied UFP emission rate for LulzBot-Laywood

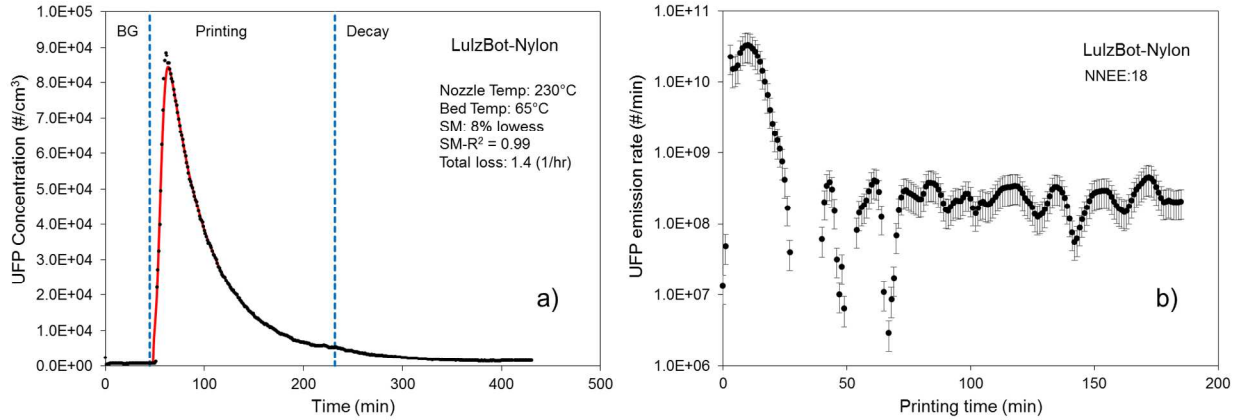

Figure S12: (a) Calibrated and smoothed UFP concentration inside the chamber and (b) Time varied UFP emission rate for LulzBot-Nylon

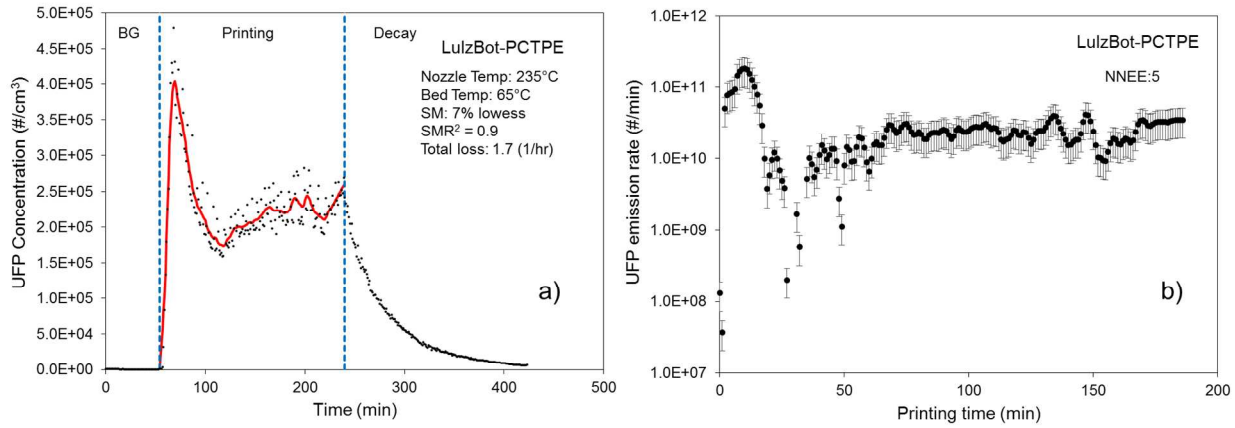

Figure S13: (a) Calibrated and smoothed UFP concentration inside the chamber and (b) Time varied UFP emission rate for LulzBot-PCTPE

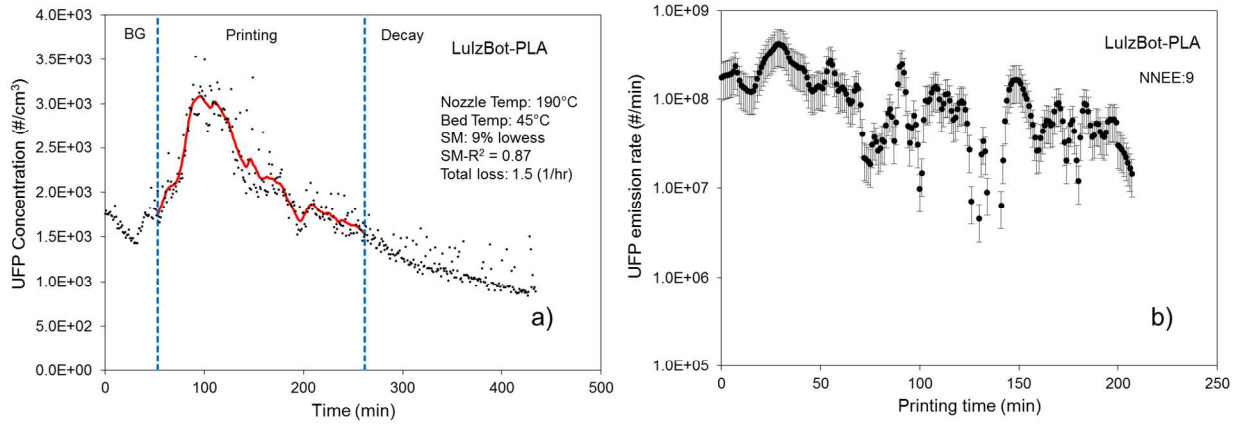

Figure S14: (a) Calibrated and smoothed UFP concentration inside the chamber and (b) Time varied UFP emission rate for LulzBot-PLA

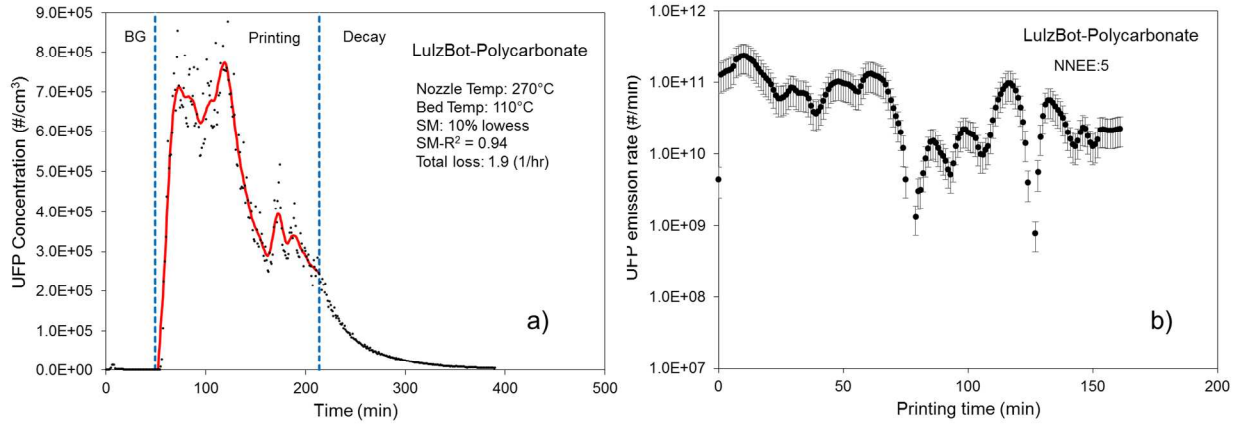

Figure S15: (a) Calibrated and smoothed UFP concentration inside the chamber and (b) Time varied UFP emission rate for LulzBot-Polycarbonate

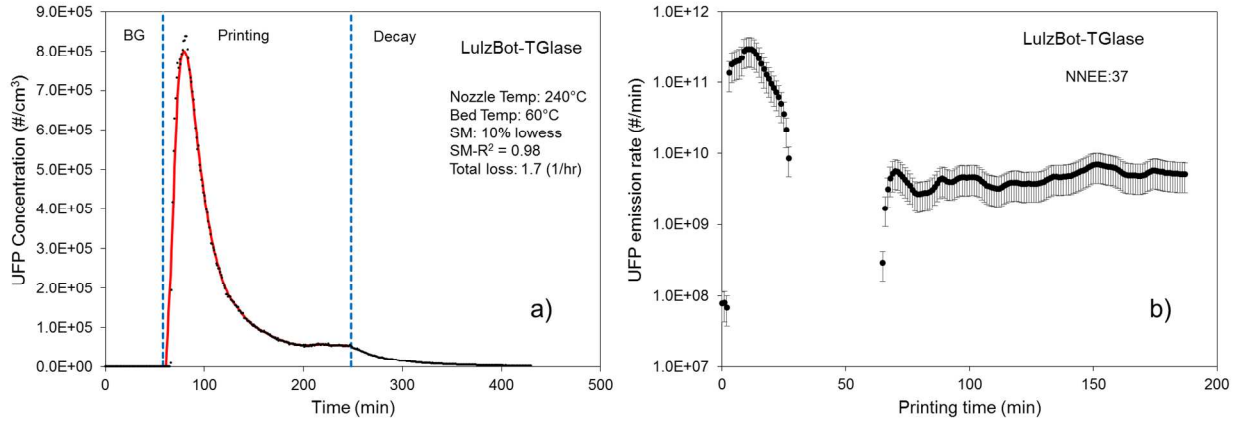

Figure S16: (a) Calibrated and smoothed UFP concentration inside the chamber and (b) Time varied UFP emission rate for LulzBot-TGlase

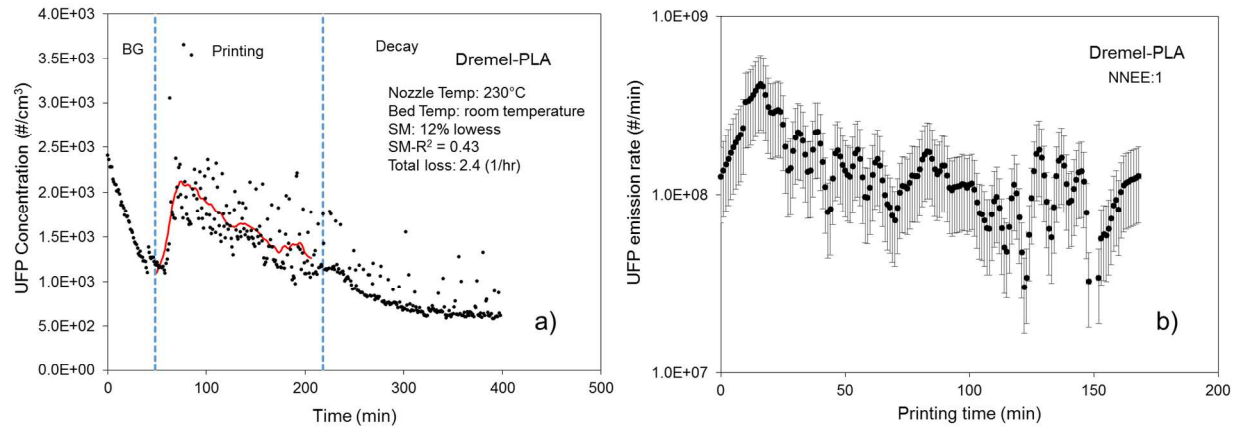

Figure S17: (a) Calibrated and smoothed UFP concentration inside the chamber and (b) Time varied UFP emission rate for Dremel-PLA

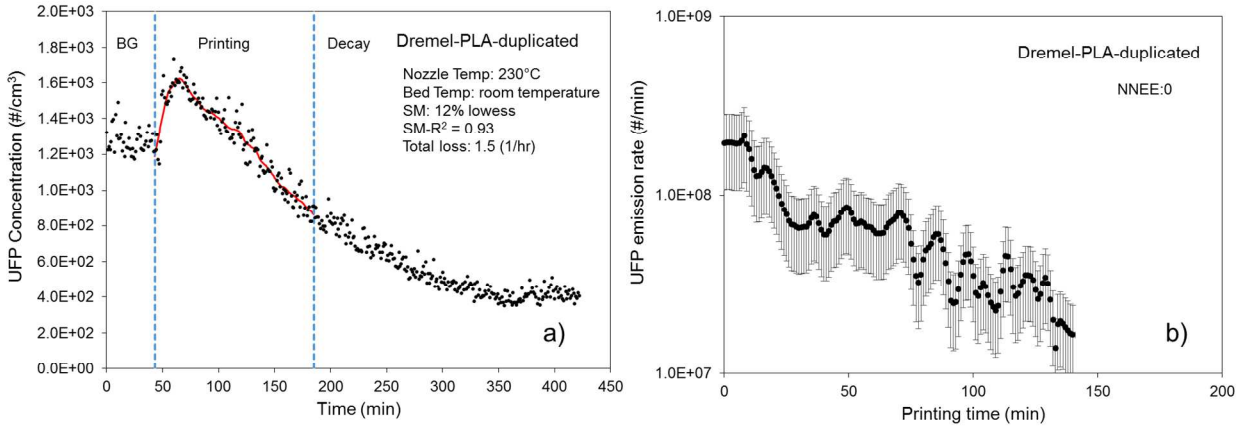

Figure S18: (a) Calibrated and smoothed UFP concentration inside the chamber and (b) Time varied UFP emission rate for Dremel-PLA (Duplicated)

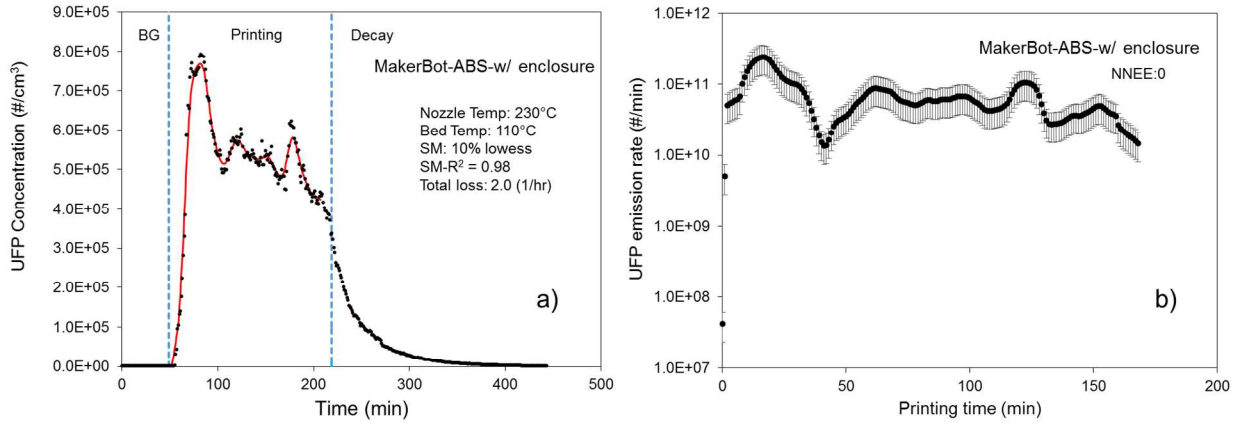

Figure S19: (a) Calibrated and smoothed UFP concentration inside the chamber and (b) Time varied UFP emission rate for Makerbot-ABS (w/ enclosure)

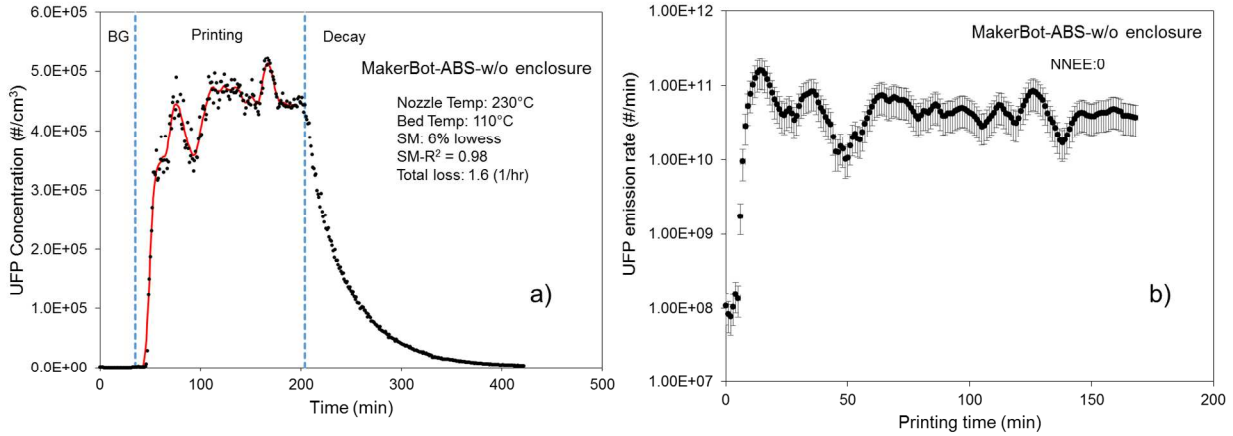

Figure S20: (a) Calibrated and smoothed UFP concentration inside the chamber and (b) Time varied UFP emission rate for Makerbot-ABS (w/o enclosure)

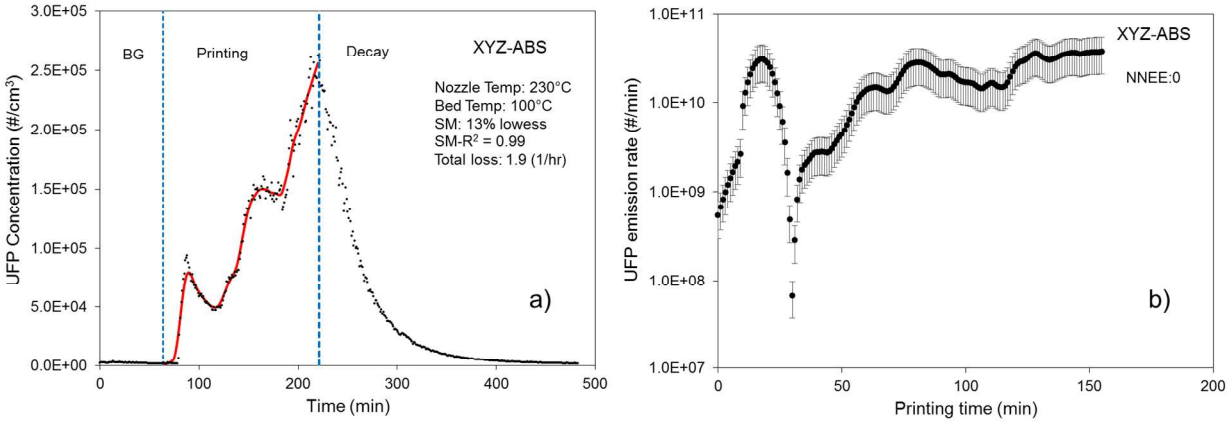

Figure S21: (a) Calibrated and smoothed UFP concentration inside the chamber and (b) Time varied UFP emission rate for XYZ-ABS

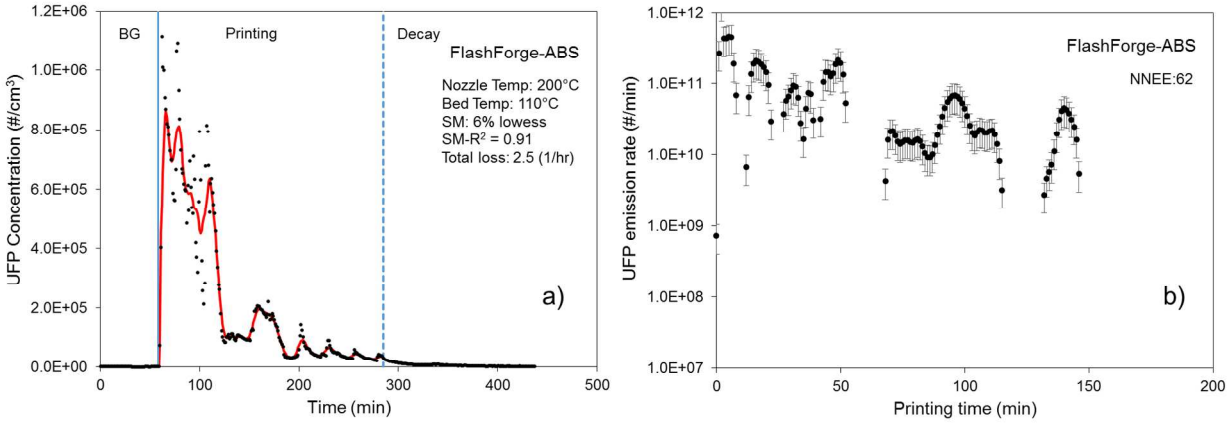

Figure S22: (a) Calibrated and smoothed UFP concentration inside the chamber and (b) Time varied UFP emission rate for FlashForge-ABS

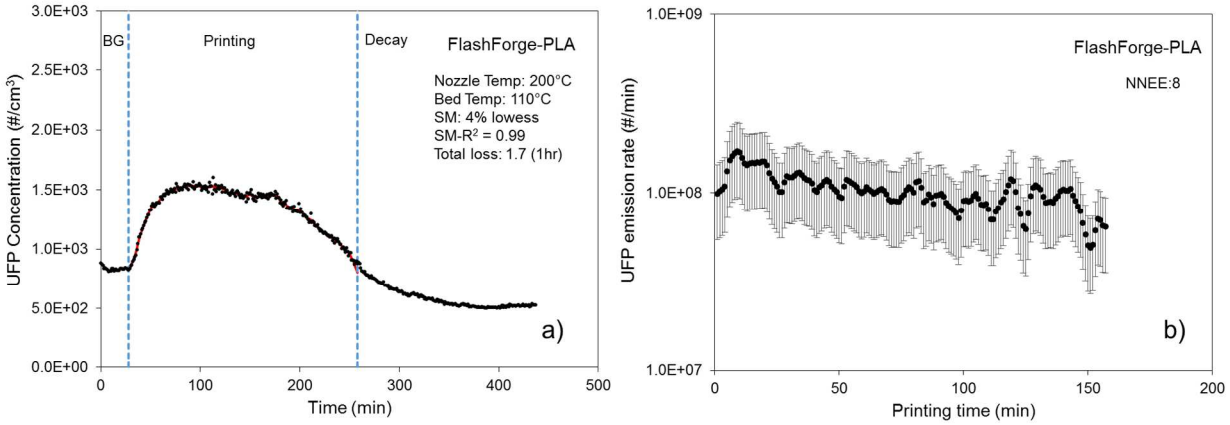

Figure S23: (a) Calibrated and smoothed UFP concentration inside the chamber and (b) Time varied UFP emission rate for FlashForge-PLA

10. VOC sampling summary

Table S2: The top 10 individual VOCs with the highest measured concentrations during printing and estimated steady-state emission rates.

	Rank	Compound name	Printing Conc. (µg/m^3)	Qual. (%)	BG Conc. (µg/m^3)	Emission rate (µg/min)
FlashForge-ABS	1	Styrene	461.0	97	0.0	33.5
	2	Propylene Glycol	158.5	64	201.5	-3.1
	3	Hexanal	135.4	90	109.2	1.9
	4	Octanal	61.1	86	55.1	0.4
	5	Nonanal	46.4	83	31.0	1.1
	6	1-Pentanol	44.1	72	48.0	-0.3
	7	Bicyclo[3.1.1]hept-2-ene, 2,6,6-tri	40.5	91	37.7	0.2
	8	Acetic acid	38.5	90	43.2	-0.3
	9	Toluene	37.8	93	89.4	-3.7
	10	Ethylbenzene	35.1	81	6.0	2.1
FlashForge-PLA	1	1,4-Dioxane-2,5-dione, 3,6-dimethyl	89.0	90	0.0	5.0
	2	Isopropyl Palmitate	79.6	93	95.6	-0.9
	3	Hexanal	39.7	90	50.4	-0.6
	4	12-Crown-4	35.1	38	0.0	2.0
	5	Nonanal	31.6	83	52.2	-1.1
	6	Octanal	30.0	86	36.8	-0.4
	7	Tetrachloroethylene	27.5	99	56.3	-1.6
	8	Benzene, 1,3-dimethyl-	24.4	95	32.5	-0.4
	9	1R-.alpha.-Pinene	21.3	95	26.8	-0.3
	10	Propylene Glycol	18.7	80	35.3	-0.9
XYZ-ABS	1	Styrene	243.2	97	0.0	11.5
	2	(S)-(+)-1,2-Propanediol (Propylene Glycol)	186.2	64	32.4	7.3
	3	Hexanal	72.9	90	55.2	0.8
	4	Glycerin	37.7	83	0.0	1.8
	5	Octanal	34.2	93	26.9	0.3
	6	1-Pentanol	31.5	72	0.0	1.5
	7	1R-.alpha.-Pinene	26.6	93	12.9	0.6
	8	Acetophenone	23.1	97	0.0	1.1
	9	Nonanal	22.3	72	22.1	0.0
	10	Decane	18.0	90	15.0	0.1
Dremel-PLA	1	Hexanal	67.4	72	88.2	-1.4
	2	1,4-Dioxane-2,5-dione, 3,6-dimethyl	53.8	90	0.0	3.7
	3	Toluene	52.9	97	87.6	-2.4
	4	Chloromethyl methyl sulfide	36.2	33	0.0	2.5
	5	Octanal	33.2	87	37.0	-0.3
	6	1-Propanol, 2-ethoxy-	29.9	42	0.0	2.1
	7	Nonanal	27.8	93	0.0	1.9
	8	2-Heptanone, 3-methyl-	26.3	9	37.0	-0.7
	9	1R-.alpha.-Pinene	25.3	96	28.7	-0.2
	10	Ethanol, 2-(2-butoxyethoxy)-	23.3	90	0.0	1.6

Table S2 continued. The top 10 individual VOCs with the highest measured concentrations during printing and estimated steady-state emission rates.

	Rank	Compound name	Printing Conc. (µg/m^3)	Qual. (%)	BG Conc. (µg/m^3)	Emission rate (µg/min)
Dremel-PLA (dupl.)	1	Hexanal	112.2	52	51.9	3.8
	2	1,4-Dioxane-2,5-dione, 3,6-dimethyl	65.6	90	21.3	2.8
	3	12-Crown-4	62.3	38	0.0	3.9
	4	Acetic acid	54.2	90	11.4	2.7
	5	Octanal	42.1	83	31.5	0.7
	6	Toluene	42.0	94	30.8	0.7
	7	Ethanol, 2-(2-butoxyethoxy)-	33.9	90	3.6	1.9
	8	1R-.alpha.-Pinene	30.9	95	32.5	-0.1
	9	Chloromethyl methyl sulfide	30.1	33	21.3	0.6
	10	Nonanal	29.4	83	23.9	0.3
LulzBot-HIPS	1	Styrene	242.3	97	13.6	19.6
	2	2-Butanone	134.8	50	131.8	0.3
	3	Toluene	109.6	94	149.9	-3.5
	4	Ethylbenzene	62.5	94	5.1	4.9
	5	Hexanal	57.7	90	35.8	1.9
	6	Octanal	43.4	91	27.1	1.4
	7	Decane	38.0	76	21.5	1.4
	8	Trimethylphosphine	36.5	33	19.5	1.5
	9	p-Xylene	30.6	95	16.0	1.2
	10	Bicyclo[3.1.1]hept-2-ene	30.1	90	23.0	0.6
LulzBot-HIPS (dupl.)	1	Styrene	212.6	97	9.6	20.7
	2	2-Butanone	81.6	50	96.6	-1.5
	3	Hexanal	55.4	90	42.8	1.3
	4	Toluene	54.5	97	65.5	-1.1
	5	Ethylbenzene	53.8	94	4.5	5.0
	6	Decane	44.7	87	31.6	1.3
	7	Acetic acid	42.9	90	13.4	3.0
	8	Octanal	39.1	91	26.6	1.3
	9	Bicyclo[3.1.1]hept-2-ene, 2,6,6-tri	30.6	91	20.8	1.0
	10	Nonanal	28.6	64	19.2	1.0
LulzBot-PLA	1	Hexanal	89.8	90	81.7	0.4
	2	1,4-Dioxane-2,5-dione, 3,6-dimethyl	79.4	90	0.0	4.4
	3	Toluene	46.9	94	46.0	0.0
	4	Octanal	45.0	94	49.5	-0.2
	5	Ethanol, 2-(2-butoxyethoxy)-	41.0	90	0.0	2.3
	6	Nonanal	38.1	86	38.2	0.0
	7	Styrene	35.4	97	12.3	1.3
	8	2-Butanone	32.4	43	64.8	-1.8
	9	Isopropyl Palmitate	30.8	96	28.0	0.2
	10	1R-.alpha.-Pinene	29.2	96	37.3	-0.4

Table S2 continued. The top 10 individual VOCs with the highest measured concentrations during printing and estimated steady-state emission rates.

	Rank	Compound name	Printing Conc. (µg/m^3)	Qual. (%)	BG Conc. (µg/m^3)	Emission rate (µg/min)
LulzBot-ABS	1	Styrene	912.8	97	8.7	54.2
	2	Hexanal	70.5	91	72.0	-0.1
	3	Acetophenone	61.5	97	0.0	3.7
	4	Ethylbenzene	59.9	87	3.4	3.4
	5	Benzenemethanol, .alpha.,.alpha.-di	44.8	72	0.0	2.7
	6	.alpha.-Pinene	42.2	64	24.0	1.1
	7	Octanal	41.4	95	39.8	0.1
	8	Toluene	40.4	94	26.4	0.8
	9	Nonanal	39.7	86	37.3	0.1
	10	1-Butanol	39.5	90	0.0	2.4
LulzBot-ABS (dupl.)	1	Styrene	919.3	97	7.4	42.7
	2	Caprolactam	272.4	94	144.9	6.0
	3	Acetophenone	70.2	97	2.8	3.2
	4	Isopropyl Palmitate	64.1	97	52.4	0.5
	5	Ethylbenzene	61.7	94	3.0	2.7
	6	Hexanal	52.5	90	67.3	-0.7
	7	Nonanal	52.1	72	33.7	0.9
	8	Octanal	46.2	90	37.1	0.4
	9	Benzenemethanol, .alpha.,.alpha.-di	44.5	80	0.0	2.1
	10	Bicyclo[3.1.1]hept-2-ene, 2,6,6-tri	44.5	89	29.6	0.7
LulzBot-ABS (cube)	1	Styrene	857.7	97	0.0	38.1
	2	Acetophenone	60.5	95	0.0	2.7
	3	Decane	58.7	94	0.0	2.6
	4	Ethylbenzene	57.3	94	24.4	1.5
	5	Isopropyl Palmitate	50.0	93	64.0	-0.6
	6	Hexanal	46.7	91	39.5	0.3
	7	Benzenemethanol, .alpha.,.alpha.-di	41.3	72	0.0	1.8
	8	Octanal	39.0	80	29.0	0.4
	9	Caprolactam	33.1	94	13.5	0.9
	10	Toluene	31.5	94	25.2	0.3
LulzBot-Nylon	1	Caprolactam	3078.3	95	35.1	182.6
	2	Hexanal	131.5	90	84.0	2.9
	3	Acetic acid	109.8	90	6.9	6.2
	4	Isopropyl Palmitate	51.1	93	21.7	1.8
	5	Octanal	50.4	83	52.4	-0.1
	6	Nonanal	50.4	83	38.3	0.7
	7	Pentanal	32.5	91	6.1	1.6
	8	1-Pentanol	32.2	59	0.0	1.9
	9	Benzyl Alcohol	30.5	93	25.8	0.3
	10	Propylene Glycol	29.2	72	29.2	0.0

Table S2 continued. The top 10 individual VOCs with the highest measured concentrations during printing and estimated steady-state emission rates.

	Rank	Compound name	Printing Conc. (µg/m^3)	Qual. (%)	BG Conc. (µg/m^3)	Emission rate (µg/min)
LulzBot-Laybrick	1	Caprolactam	1321.7	95	13.5	69.1
	2	Hexanal	110.2	91	103.1	0.4
	3	Acetic acid	61.4	90	16.8	2.4
	4	Octanal	60.0	80	52.4	0.4
	5	2-Hexenal, 2-ethyl-	58.6	93	0.0	3.1
	6	Isopropyl Palmitate	54.8	59	65.5	-0.6
	7	Nonanal	50.8	72	48.3	0.1
	8	1-Pentanol	47.1	64	39.6	0.4
	9	1R-.alpha.-Pinene	44.0	96	41.8	0.1
	10	Styrene	39.3	96	7.4	1.7
LulzBot-Laywood	1	Caprolactam	1128.6	95	33.0	45.4
	2	2-Hexenal, 2-ethyl-	96.9	86	0.0	4.0
	3	Hexanal	94.9	90	94.7	0.0
	4	Octanal	53.4	95	54.1	0.0
	5	Nonanal	46.8	64	60.9	-0.6
	6	Acetic acid	46.5	90	10.6	1.5
	7	1-Pentanol	35.5	78	36.6	0.0
	8	Isopropyl Palmitate	32.2	52	43.5	-0.5
	9	1R-.alpha.-Pinene	31.7	96	36.2	-0.2
	10	1,3,5,7-Cyclooctatetraene	31.2	97	10.1	0.9
LulzBot-TGlase	1	Caprolactam	72.8	95	30.0	1.5
	2	Hexanal	59.2	90	59.1	0.0
	3	Toluene	36.2	94	29.5	0.2
	4	Octanal	36.2	91	43.0	-0.2
	5	Nonanal	30.9	59	41.3	-0.4
	6	1R-.alpha.-Pinene	25.1	96	34.1	-0.3
	7	1-Pentanol	24.2	78	32.3	-0.3
	8	Styrene	22.1	97	9.7	0.4
	9	R-(-)-1,2-propanediol (Propylene Glycol)	22.0	80	5.4	0.6
	10	Isopropyl Palmitate	21.0	97	19.8	0.0
LulzBot-Polycarbonate	1	Propylene Glycol	141.6	64	257.5	-3.7
	2	Caprolactam	82.9	95	37.3	1.5
	3	Toluene	78.6	94	89.6	-0.3
	4	Hexanal	68.4	90	69.9	0.0
	5	Isopropyl Palmitate	58.6	93	63.1	-0.1
	6	Octanal	53.3	96	60.0	-0.2
	7	1R-.alpha.-Pinene	47.4	95	55.4	-0.3
	8	1-Pentanol	43.7	64	45.4	-0.1
	9	Styrene	42.6	97	21.1	0.7
	10	Nonanal	42.5	83	54.0	-0.4

Table S2 continued. The top 10 individual VOCs with the highest measured concentrations during printing and estimated steady-state emission rates.

	Rank	Compound name	Printing Conc. (µg/m^3)	Qual. (%)	BG Conc. (µg/m^3)	Emission rate (µg/min)
LulzBot-Polycarbonate (dupl.)	1	Isopropyl Palmitate	77.1	93	138.9	-3.0
	2	Decanal	64.6	87	0.0	3.2
	3	Hexanal	51.0	90	21.6	1.4
	4	Nonanal	49.1	83	29.4	1.0
	5	Octanal	49.0	83	22.2	1.3
	6	Tetrachloroethylene	47.5	99	113.9	-3.3
	7	Phenol	40.1	96	0.0	2.0
	8	Caprolactam	34.5	93	5.5	1.4
	9	1-Pentanol	31.1	43	0.0	1.5
	10	1R-.alpha.-Pinene	30.3	96	15.4	0.7
LulzBot-PCTPE	1	Caprolactam	4940.0	95	30.1	167.9
	2	Isopropyl Palmitate	72.2	58	41.0	1.1
	3	Hydrazinecarbothioamide	38.2	9	7.9	1.0
	4	Nonanal	37.5	83	19.8	0.6
	5	Styrene	23.2	97	5.7	0.6
	6	Silane, trimethyl(1-methylethoxy)-	20.6	59	0.0	0.7
	7	2-Hexene, 3,5,5-trimethyl-	20.5	43	3.8	0.6
	8	Octanal	18.0	91	10.0	0.3
	9	Hexanal	16.7	86	10.6	0.2
	10	1R-.alpha.-Pinene	15.4	96	11.9	0.1
MakerBot-w/-enclosure	1	Styrene	2478.7	97	0.0	113.0
	2	Acetophenone	164.4	95	0.0	7.5
	3	Isopropyl Palmitate	139.6	93	0.0	6.4
	4	Tetrachloroethylene	130.1	99	8.5	5.5
	5	Decane	127.8	94	0.0	5.8
	6	dl-2-Phenyl-1,2-propanediol	120.6	64	0.0	5.5
	7	Ethylbenzene	119.3	94	0.0	5.4
	8	Cyclotrisiloxane, hexamethyl-	117.0	83	0.0	5.3
	9	Benzeneethanamine, N-[(pentafl	89.0	32	0.0	4.1
	10	1-Butanol	87.7	78	0.0	4.0
MakerBot-w/o-enclosure	1	Styrene	1632.7	97	10.8	96.3
	2	Isopropyl Palmitate	207.3	96	48.4	9.4
	3	Nonane, 2,2,4,4,6,8,8-heptamet	122.8	83	0.0	7.3
	4	Acetophenone	118.3	95	3.9	6.8
	5	Chloromethyl methyl sulfide	89.5	33	0.0	5.3
	6	Benzenemethanol, .alpha.,.alph	81.3	64	0.0	4.8
	7	Nonanal	80.7	72	62.1	1.1
	8	Ethylbenzene	78.4	94	7.6	4.2
	9	Cyclotrisiloxane, hexamethyl-	75.8	87	13.0	3.7
	10	Benzeneethanamine, N-[(pentafl	59.9	37	0.0	3.6

Table S2 continued. The top 10 individual VOCs with the highest measured concentrations during printing and estimated steady-state emission rates.

	Rank	Compound name	Printing Conc. (µg/m^3)	Qual. (%)	BG Conc. (µg/m^3)	Emission rate (µg/min)
LulzBot without filament with applying on bed*	1	(S)-(+)-1,2-Propanediol	408.5	93	210.9	N/A‡
	2	Glycerin	199.4	87	0.0	N/A
	3	Hexanal	98.1	90	65.8	N/A
	4	Benzene, 1,3-dimethyl-	85.4	83	97.7	N/A
	5	Acetic acid	62.9	83	34.6	N/A
	6	Octanal	51.6	99	34.6	N/A
	7	Isopropyl Palmitate	39.8	96	59.2	N/A
	8	1-Pentanol	37.1	93	29.9	N/A
	9	Nonanal	35.5	43	30.0	N/A
	10	Heptanal	32.8	96	0.0	N/A

* We operated the 3D printer without any filament to characterize the individual VOC compounds emitted from the glue applied on the 3D printer bed, as glue was used in several normal printing tests to ensure that the printed piece adhered to the platform.

‡ We did not estimate emission rates because we could not confirm whether or not VOC concentrations reached to steady state levels when the printer was operated without filament (the duration of printing was short: about 45 mins).

Table S3: Top 10 individual VOCs with the highest measured concentrations outside the chamber

	Rank	Outside the chamber			Rank	Outside the chamber	
		Compound name	Conc. (µg/m^3)			Compound name	Conc. (µg/m^3)
LulzBot-ABS	1	Decane	0.02	LulzBot-ABS (dupl.)	1	Furfural	0.02
	2	Phenylethanolamine	0.02		2	Benzaldehyde	0.01
	3	Ethanol, 2-(2-ethoxyethoxy)-	0.01		3	Nonanal	0.01
	4	Nonane	0.01		4	n-Hexadecanoic acid	0.01
	5	Furfural	0.01		5	Tetrasiloxane, 1,1,3,3,5,5,7,7-octa	0.01
	6	Acetophenone	0.01		6	1-Propanol, 3-phenoxy-	0.01
	7	Undecane	0.01		7	Decane	0.01
	8	Decanal	0.01		8	Butanoic acid, 3-methylbutyl ester	0.01
	9	2-Butanone	0.01		9	Benzene, 1,2,3-trimethyl-	0.01
	10	Nonanal	0.01		10	Octanal	0.01
MakerBot-w/-enclosure	1	Isopropyl Palmitate	0.02	MakerBot-w/o-enclosure	1	Benzene, 1,3-dimethyl-	0.02
	2	Benzene, 1,3-dimethyl-	0.02		2	Isopropyl Palmitate	0.02
	3	Nonane, 2,2,4,4,6,8,8-heptamethyl-	0.02		3	Acetophenone	0.02
	4	Acetophenone	0.01		4	Nonanal	0.01
	5	Chloromethyl methyl sulfide	0.01		5	Benzene, 1,2,4-trimethyl-	0.01
	6	Nonanal	0.01		6	Octanal	0.01
	7	Decane	0.01		7	Tetrachloroethylene	0.01
	8	Octanal	0.01		8	Hexanal	0.01
	9	Hexanal	0.01		9	Benzene, 1,3,5-trimethyl-	0.01
	10	Toluene	0.01		10	Benzyl Alcohol	0.01

11. Validating the discretized UFP emission rate solution

In a few scenarios, UFP concentrations reach an approximately steady state level towards the end of printing period. We estimated the UFP emission rate during these time periods using a simple number balance equation as shown Equation S24.

$$\frac{E_{UFP,ss}}{VL_{UFP}} = C_{UFP,in,ss} - \frac{P_{UFP}\lambda C_{UFP,out}}{L_{UFP}} \quad \text{(S24)}$$

$C_{UFP,in,ss}$= UFP steady state concentration inside the chamber during the selected time period (#/cm^3)

$E_{UFP,ss}$= UFP steady state emission rate during the selected time period (#/min)

As previously mentioned, $\frac{P_{UFP}\lambda C_{UFP,out}}{L_{UFP}}$ is equal to average measured background concentration ($\bar{C}_{UFP,bg}$) and the total UFP loss rate (L_{UFP}) can be estimated from the final decay period after printing was stopped using a log-linear regression solution. We validated our method for estimating UFP emission rates by comparing the results from Equation S24 to average estimated UFP emission rates from discretized solution method (Equation S7 in Section 5). Five combinations of 3D printer and filament were selected for this comparison including LulzBot-ABS, LulzBot-PCTPE, LulzBot-TGlase, MakerBot-ABS with enclosure, and FlashForge-PLA. The summary of steady state time periods, estimated steady state UFP emission rates ($E_{UFP,ss}$), and the average estimated UFP emission rates using the discretized solution method ($\bar{E}_{UFP,ss}$) are listed in Table S4.

Table S4: Estimated UFP emission during steady state time periods using the simple mass balance model and the discretized solution method

Printer	*Filament*	*Time period (minutes after start printing)*	L_{UFP} *(1/min)*	$\bar{C}_{UFP,bg}$ *(#/cm^3)*	$C_{UFP,in,ss}$ *(#/cm^3)*	$E_{UFP,ss}$ *(#/min)*	$\bar{E}_{UFP,ss}$ *(#/min)*	*Difference (%)*
LulzBot	ABS	80-115	0.0354	1,166	722,395	9.19×10^{10}	9.69×10^{10}	5.5
	PCTPE	85-170	0.0281	429	222,012	2.24×10^{10}	2.33×10^{10}	3.7
	TGlase	140-180	0.029	931	56,401	5.79×10^{9}	5.71×10^{9}	1.4
MakerBot w/ enclosure	ABS	75-100	0.0333	1,214	535,999	6.41×10^{10}	5.99×10^{10}	6.6
FlashForge	PLA	60-140	0.028	523	1,487	9.72×10^{7}	9.38×10^{7}	3.6

The difference between estimated UFP emission rates using the steady state mass balance model and the discretized solution method remains under 7% for the 5 chosen 3D printer and filament combinations. Giving that the uncertainty around the estimated UFP emission rate is ~45%, the results demonstrate that there is no meaningful difference between UFP emission estimations from these two methods, which shows that the dynamic solution method used herein is reasonable.

12. Additional references

(1) Won, D.; Corsi, R. L.; Rynes, M. Sorptive Interactions between VOCs and Indoor Materials. *Indoor Air* **2001**, *11* (4), 246–256.

(2) Cox, S. S.; Little, J. C.; Hodgson, A. T. Predicting the Emission Rate of Volatile Organic Compounds from Vinyl Flooring. *Environ. Sci. Technol.* **2002**, *36* (4), 709–714.

(3) Hinds, W. C. *Aerosol technology: properties, behavior, and measurement of airborne particles*; John Wiley & Sons, 2012.

(4) Stephens, B.; Azimi, P.; Orch, Z. El; Ramos, T. Ultrafine particle emissions from desktop 3D printers. *Atmos. Environ.* **2013**, *79*, 334–339.